Resonantly Enhanced Above-Threshold Ionization of Helium

M. D. Perry, A. Szoke, and K. C. Kulander
Lawrence Livermore National Laboratory, P.O. Box 808, L-473, Livermore, California 94550
(Received 10 March 1989)

The role of multiphoton resonances in the above-threshold ionization of helium at intensities above 10^{14} W/cm^2 is investigated by both theory and experiment from 280 to 297 nm. Strong enhancement is observed in above-threshold ionization electron spectra and is attributed to five- and six-photon resonances to the $1s2p$ and $1s3d$, respectively. Numerical solution of the time-dependent Schrödinger equation predicts asymmetric resonance profiles with positions and ionization rates which are in good agreement with experiment.

PACS numbers: 32.80.Rm, 42.50.Hz

In this paper, we present the systematic theoretical and experimental study of resonant enhancement in strong field, above-threshold ionization (ATI) of helium. The study is the first to examine the ATI electron spectrum as a function of both laser intensity *and* frequency with subpicosecond, tunable ultraviolet laser radiation at intensities above 10^{14} W/cm^2.

The recent success of theories which connect only the ground atomic state to an outgoing dressed electron state[1,2] in predicting ionization rates[3] and (ATI) electron spectra[4] suggest that resonances to intermediate atomic states, if they occur during the laser pulse, do not significantly affect the ionization rate. Conversely, observations by Freeman *et al.*[5] and others[6] of fine structure in electron spectra produced by the ATI of xenon at 616 nm using subpicosecond pulses suggest that intermediate resonances remain important even at intensities greater than 10^{14} W/cm^2. Such resonances may play an important role in the production of high-order harmonic radiation in strong fields.[7,8]

By examining the ATI electron spectrum obtained with "short" laser pulses as a function of both frequency and intensity, the identity of any such intermediate resonance can be determined as well as the ac Stark shift of the state.[9] Helium is of particular interest for several reasons. First, its simple structure permits detailed calculations. Second, it provides two strong intermediate resonances, $1s^2+5\hbar\omega \rightarrow 1s2p$ and $1s^2+6\hbar\omega \rightarrow 1s3d$, which are well separated from other states and bound by at least 1.5 eV. This removes much of the ambiguity associated with examining resonances to states near the continuum.[5]

Photoelectrons resulting from above-threshold ionization are born with a kinetic energy,[10]

$$E_e = (K+S)\hbar\omega - \phi_{\mathrm{IP}}(I) = (K+S)\hbar\omega - \phi_{\mathrm{IP}}(0) - U_p(I), \quad (1)$$

where K is the minimum number of photons which must be absorbed to ionize the atom in the absence of the field, and S is the number of additional (ATI) photons absorbed. The ionization threshold, ϕ_{IP}, is intensity dependent to account for the quiver energy of the newly freed electron in the field. This quiver or "ponderomotive" energy is given by $U_p = e^2A^2/4mc^2 = 9.33\times10^{-14}\times I\lambda^2$ eV, where I is the laser intensity in W/cm^2 and λ is the wavelength of the laser light in microns. The difference in the dynamic Stark shifts of the atomic and ionic ground states is not included in Eq. (1) since it is negligible relative to the quiver energy of the electron.

If the duration of the laser pulse is shorter than the time required for the electron to leave the laser focus, then the conversion of potential to kinetic energy is incomplete and results in an intensity-dependent deficit in the kinetic energy. In the limit that the pulse is infinitely short, the electron energy detected is equal to the energy with which the electron is born [Eq. (1)], and hence *records the intensity present at the moment of ionization.* The short-pulse regime is approached with subpicosecond lasers.[5,6,11]

The electron spectrometer used in these experiments collects all electrons emitted within the 2π solid angle in the direction of the microchannel-plate detector.[12] The energy of a given photoelectron is determined by its time of flight down a 50-cm drift tube. The spectrometer was calibrated utilizing the photoelectron spectrum resulting from the above-threshold ionization of xenon and helium at 532 nm with long (70-psec) pulses.[4]

The laser system used is described in detail elsewhere.[13] Amplified, Fourier-transform limited pulses with widths between 0.7 and 1 psec are obtained over the range 560 to 595 nm. These pulses were frequency doubled in a 5-mm-thick potassium dihydrogen phosphate (KDP) crystal providing tunable radiation from 280 to 297 nm with pulses typically 0.6 to 0.8 psec in duration.

The ultraviolet pulses were focused into low-density helium gas with a 45-mm focal length fused silica lens ($f=5$) to a slightly astigmatic spot of approximately 10 μm diam. The experiments were conducted in a range of helium pressure between 4×10^{-7} and 4×10^{-6} Torr. The pressure was decreased as the laser intensity was increased in order to avoid space-charge distortion of the

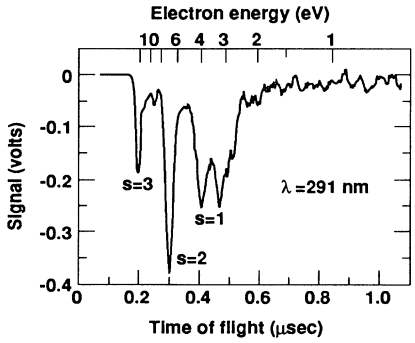

FIG. 1. Electron spectrum resulting from the above-threshold ionization of helium at 291 nm and a peak intensity of 4×10^{14} W/cm^2.

spectrum.[14] A typical time-of-flight spectrum at a peak laser intensity of 4×10^{14} W/cm^2 and 291 nm is shown in Fig. 1. Electrons corresponding to the absorption of seven ($s=1$), eight ($s=2$), and nine ($s=3$) photons can be observed at this intensity. At higher intensities, electrons corresponding to the absorption of ten photons could be observed. Electrons corresponding to threshold ionization ($s=0$) could be produced only from regions of intensity less than 1.2×10^{14} W/cm^2 [Eq. (1)] and are not observed at this wavelength. Electrons corresponding to $s=1$ clearly come in two distinct energy groups indicating electrons produced at different intensities.

Figure 2 contains data taken at 281.5 nm in the region from 2 to 9 eV for several values of peak laser intensity. The averaged spectra shown in Figs. 2(a)–2(e) are acquired by sorting the spectra of several hundred laser shots into narrow bins of differing electron yield. Since the yield is a strong function of laser intensity, this method results in sets of spectra averaged over a narrow intensity interval.[15] The 2–9-eV region covers the $s=2$ peak near 7.5 eV and the $s=1$ peak between 2.5 and 4 eV. These peaks are clearly shifted from the field-free positions of 6.24 and 10.6 eV which would have been obtained with "long" laser pulses. At the lower intensities, the electron spectrum exhibits single peaks corresponding to the absorption of seven ($s=1$) and eight ($s=2$) photons. As the laser intensity increases, some of the $s=1,2$ electrons are observed with decreasing energy. At a peak intensity of 4×10^{14} W/cm^2, a clear second peak appears which is apparently part of the $s=1$ peak. Similar substructure in the $s=2$ peak is observed by acquiring the $s=2$ electrons under higher-energy resolution (not shown). As the intensity is raised further, the yield of electrons to this secondary peak increases but its position does not shift towards lower energy as does the primary part of the $s=1$ peak.

The secondary peak apparently arises from a region of laser intensity appropriate to shift a state into resonance with an integral number of 4.4-eV photons (281.5 nm). The ionization probability in this region is enhanced relative to the nonresonant probability by the intermediate resonance. Since the intensity at which the electron is produced determines its energy [Eq. (1)], those electrons produced from resonant enhancement will always appear at the same energy regardless of the value of the peak laser intensity.

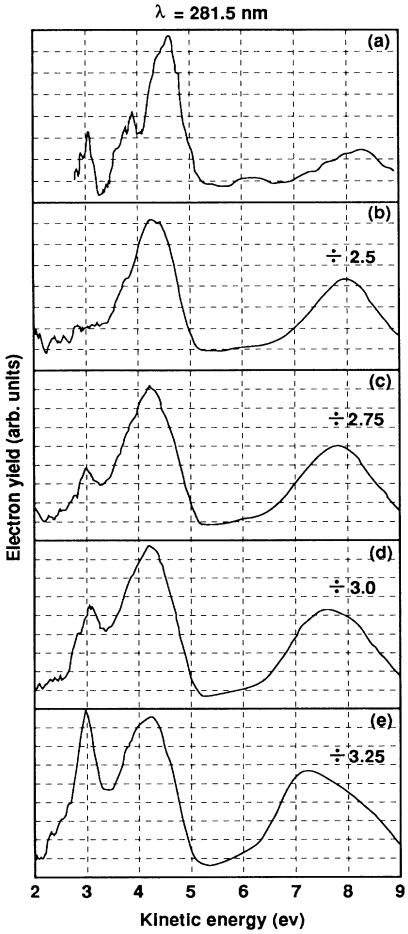

FIG. 2. Electron-energy distribution obtained at 281.5 nm ($s=1$ and $s=2$ peaks only) at various laser intensities (units of 10^{14} W/cm^2): (a) $I_0=3.1$, (b) 3.6, (c) 3.8, (d) 4.3, and (e) 4.4. Data below 3.5 eV in (a) are not statistically significant. The change in the vertical scale is given by the factor at the right-hand side of each figure.

Examination of the positions of the field-free singlet states in helium[16] suggests that the enhancement observed in the $s=1$ peak is due to a six-photon resonance to the $1s3d$ state. At 281.5 nm, this state would have to be shifted towards higher energy by 3.3 eV to be resonant. This was confirmed by acquiring electron spectra at several wavelengths in the range 280 to 297 nm. Longer wavelength light requires less of a shift and results in the appearence of the resonance at lower laser intensity (Figs. 3 and 4). Hence, the position of the resonance as a function of intensity can be traced by tuning

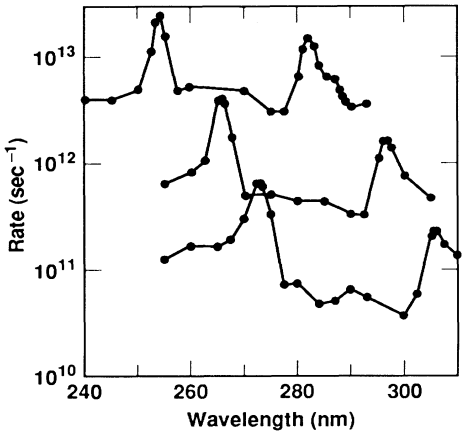

FIG. 3. Ionization rates for helium as a function of laser wavelength obtained from the numerical solution of the time-dependent Schrödinger equation at 2×10^{14}, 3×10^{14}, and 5×10^{14} W/cm^2.

the laser frequency. At the shortest wavelengths, a second resonance corresponding to five-photon excitation of the $1s2p$ was observed.

To provide further insight to the experimental data, we developed a nonperturbative theoretical description of helium subjected to these strong fields. We solve the atom-field Schrödinger equation by direct numerical integration for an adiabatic pulse. The laser pulse rises linearly over several optical cycles and is then held constant at the prescribed intensity. During the constant-intensity interval, the atom is found to decay exponentially thereby giving an ionization rate for the particular intensity and wavelength. The model of the helium atom used here[17] allows only one of the two electrons to interact with the field. The second electron is held frozen in its ground (Hartree-Fock) orbital.

We performed a series of calculations at selected values of the laser intensity as a function of wavelength between 240 and 320 nm. The calculated ionization rates are shown in Fig. 3. On each curve, two strong features are evident, the strongest is a result of five-photon resonance with a state arising from the $1s2p$ and the other a result of six-photon excitation of a state arising from the $1s3d$. Projection of these wave functions onto the field-free states shows that these states are no longer pure $1s2p$ ($1s3d$) but are strongly mixed by the field. Both states shift towards higher energy with increasing laser intensity and exhibit a width which is dominated by the short lifetime of these excited states at intensities above 10^{14} W/cm^2. The absolute positions of the resonances must be corrected for the difference between the experimentally determined field-free positions of the $1s2p$ (21.21 eV) and $1s3d$ (23.07 eV) and those calculated by our Hartree-Fock model, 20.76 and 22.74 eV, respectively. Note that the calculated resonance profiles are asymmetric indicating interference between

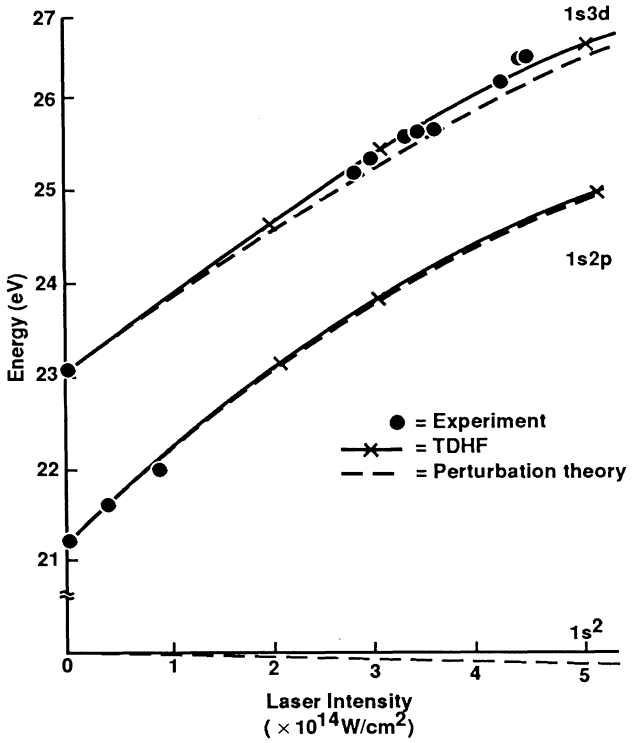

FIG. 4. Energy of states arising from the $1s2p$ and $1s3d$ field-free singlet states of helium as a function of laser intensity. The dashed curve originating at zero energy for the $1s^2$ emphasizes the shift of the ground state to lower energy with increasing intensity.

the resonant and nonresonant ionization paths. This is a feature which to our knowledge has not been previously observed in nonperturbative calculations of multiphoton ionization in strong fields.

The calculated and experimental energy of the $1s2p$ and $1s3d$ states is shown as a function of laser intensity in Fig. 4. The energy of the state is determined by the laser frequency at which five ($1s2p$) or six ($1s3d$) photons result in resonant enhancement. The experimental intensity at which the resonance occurs is determined from the electron spectra as discussed previously. The solid curve represents the results of our numerical solution to the Schrödinger equation. For comparison, we have also carried out a lowest-order perturbation-theory calculation (corrected to account for the changing laser wavelength) for the energy of both the ground and excited states (dashed curve). Both the numerical and perturbation-theory calculations of the resonance positions reproduce the experimental data within a few percent over the range of intensity investigated.

Ionization rates obtained from the electron yield to each ATI peak were generally found to be slightly higher than our time-dependent Hartree-Fock (TDHF) calculated rates but lower than those from our modified version[3] of the Keldysh-Reiss-Faisal (KRF) theory.

Specifically, at an intensity of 3×10^{14} W/cm^2 and wavelength of 294 nm, we calculate an ionization rate of 1.5×10^{12} sec^{-1} for six-photon resonant ($1s3d$), seven-photon ($s=1$) ionization, while experiment yields a value of $(3\pm1)\times10^{12}$ sec^{-1}. For "nonresonant" seven-photon ionization at this intensity and wavelength, we calculate rates of $(3\pm1)\times10^{11}$ sec^{-1} (TDHF) and 2.5×10^{12} sec^{-1} (KRF), but measure a rate of $(1.5\pm0.8)\times10^{12}$ sec^{-1}. The apparent uncertainty in the numerical (TDHF) calculations for the nonresonant ionization is a result of some definite, but comparatively weak, structure between the two main resonances (Fig. 3). We attribute this weak structure to six-photon resonances through the Rydberg states, a feature which may become more pronounced at lower intensities. It is important to note that the primary part of the $s=1$ peak in the electron yield discussed earlier (Fig. 2) may in fact be the result of resonances to these Rydberg states.

Our calculations also predict significant enhancement of harmonic radiation near both observed resonances.[18] Also, the highest predicted harmonic frequency corresponds to the highest experimentally observed ATI peak as proposed by Eberly, Su, and Javanainen.[19]

In conclusion, we have demonstrated that intermediate multiphoton resonances can play a significant role in above-threshold ionization even at intensities exceeding 10^{14} W/cm^2. The effect of the resonance is manifest in the ATI photoelectron energy spectrum obtained with short pulses as first suggested by Freeman. By measuring the electron spectra as a function of both laser intensity *and* frequency, the intensity-dependent position of the intermediate states can be determined as well as ionization rates through these states. A numerical solution of the time-dependent Schrödinger equation for a single-electron atomic model provides ionization rates and resonance positions which are in good agreement with experiment. The calculations show that at these intensities, the intermediate states no longer exhibit their pure, field-free character but are instead severely mixed and may exhibit an asymmetric profile. Surprisingly, we find that the resonance *positions* in these strong fields are also well described by perturbation theory.

We would like to acknowledge the technical assistance of Neil Hinsey and helpful discussions with S. Dixit, O. L. Landen, P. H. Bucksbaum, and R. R. Freeman.

[1]L. V. Keldysh, Zh. Eksp. Teor. Fiz. **47**, 1945 (1965) [Sov. Phys. JETP **20**, 1307 (1965)].

[2]F. H. M. Faisal, J. Phys. B **6**, L89 (1973); H. R. Reiss, Phys. Rev. A **22**, 1786 (1980).

[3]M. D. Perry, A. Szoke, O. L. Landen, and E. M. Campbell, Phys. Rev. Lett. **60**, 1270 (1988); S. L. Chin, C. Rolland, P. B. Corkum, and P. Kelly, Phys. Rev. Lett. **61**, 153 (1988).

[4]P. H. Bucksbaum, M. Bashkansky, and D. W. Schumacher, Phys. Rev. A **37**, 3615 (1988).

[5]R. R. Freeman, P. H. Bucksbaum, H. Milchberg, S. Darack, D. Schumacher, and M. E. Geusic, Phys. Rev. Lett. **59**, 1092 (1987).

[6]H. G. Muller, H. B. van Linden van de Heuvell, P. Agostini, G. Petite, A. Antonetti, M. Franco, and A. Migus, Phys. Rev. Lett. **60**, 565 (1988).

[7]M. Ferray, A. L'Hullier, X. F. Li, L. A. Lompre, G. Mainfray, and C. Manus, J. Phys. B **21**, L31 (1988).

[8]K. C. Kulander and B. W. Shore, Phys. Rev. Lett. **62**, 524 (1989).

[9]A. Szoke, J. Phys. B **21**, L125 (1988); A. Szoke, O. L. Landen, and M. D. Perry, Lawrence Livermore National Laboratory Report No. UCRL 99422, 1988 (to be published).

[10]A. Szoke, J. Phys. B **18**, L427 (1985).

[11]T. S. Luk, T. Graber, H. Jara, U. Johann, K. Boyer, and C. K. Rhodes, J. Opt. Soc. Am. B **4**, 847 (1987).

[12]P. Kruit and F. H. Read, J. Phys. E **16**, 313 (1983).

[13]M. D. Perry, O. L. Landen, J. Weston, and R. Ettelbrick, Opt. Lett. **14**, 42 (1989).

[14]M. Crance, J. Phys. B **19**, L267 (1986).

[15]M. D. Perry, O. L. Landen, and A. Szoke, J. Opt. Soc. Am. B **6**, 344 (1989).

[16]S. Bashkin and J. O. Stoner, *Energy Levels and Groatrian Diagrams* (North-Holland, New York, 1975).

[17]K. C. Kulander, Phys. Rev. A **36**, 2726 (1987).

[18]K. C. Kulander, M. D. Perry, and S. Dixit (to be published).

[19]J. Eberly, Q. Su, and J. Javanainen, Phys. Rev. Lett. **62**, 881 (1989).